Electronic Supplementary Material (ESI) for Chemical Science.

Enabling Al Sacrificial Anode in Tetrahydrofuran Electrolytes for Reductive Electrosynthesis

Wendy Zhang,[†] Weiyang Guan,[‡] Yi Wang,[‡] Song Lin,[‡] and Kimberly A. See[*,†]

†*Division of Chemistry and Chemical Engineering, California Institute of Technology, Pasadena, California 91125, United States*

‡*Department of Chemistry and Chemical Biology, Cornell University, Ithaca, New York 14853, United States*

E-mail: ksee@caltech.edu

Supporting Information

Linear sweep voltammograms of Al stripping

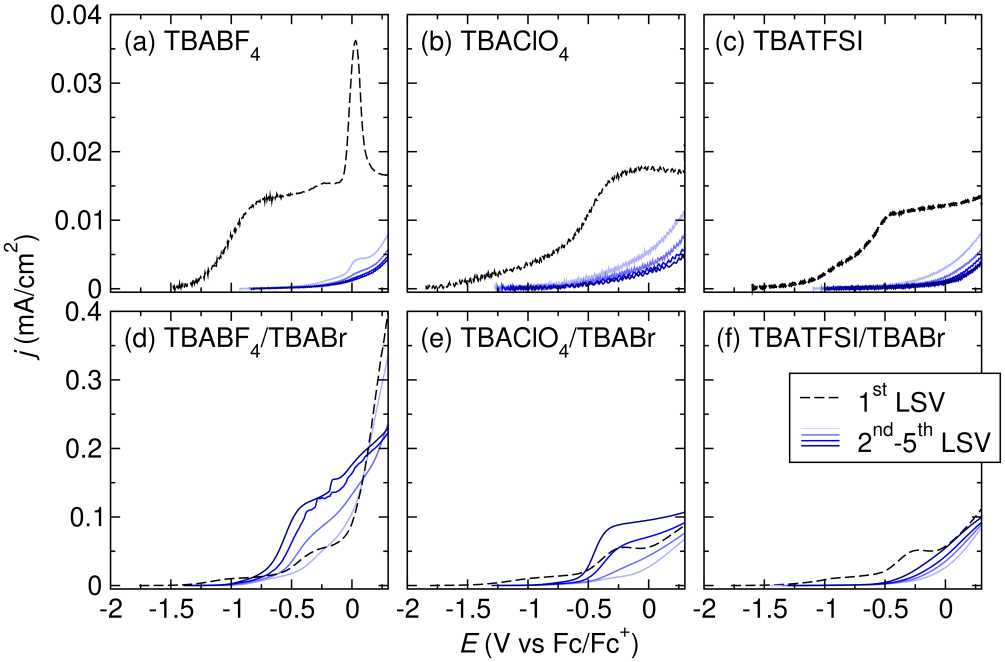

Figure S1: Linear sweep voltammograms of Al stripping in THF with 0.1 M TBA^+ supporting electrolyte or 0.05 M TBA^+ supporting electrolyte of interest + 0.05 M TBABr . All voltammograms were collected at a scan rate of 5 mV s^{-1} with 85% iR compensation. For each electrolyte, five LSVs were collected with a 10 min OCV between scans.

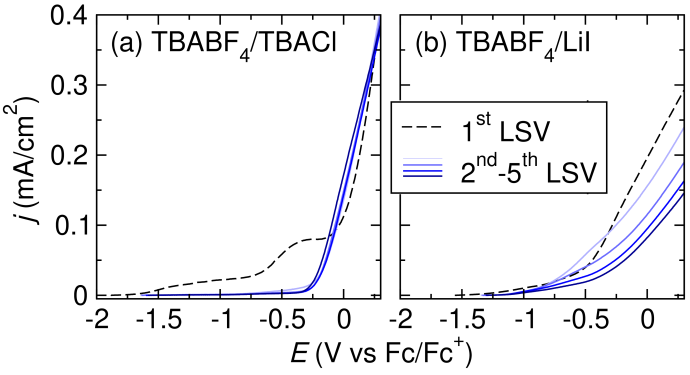

Figure S2: Linear sweep voltammograms of Al stripping in THF with 0.05 M $TBABF_4$ + 0.05 M TBACl or TBAI . All voltammograms were collected at a scan rate of 5 mV s^{-1} with 85% iR compensation. For each electrolyte, five LSVs were collected with a 10 min OCV between scans.

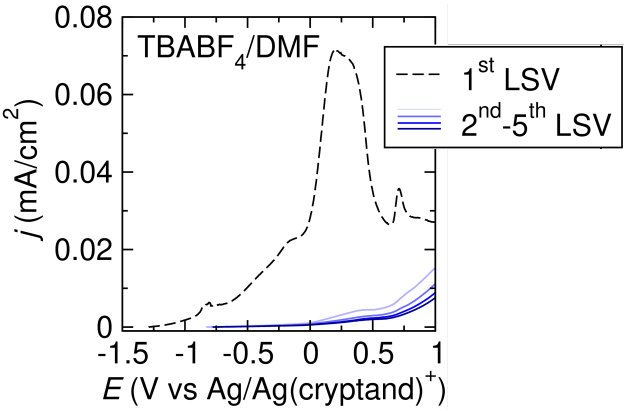

Figure S3: Linear sweep voltammograms of Al stripping in DMF with 0.1 M $TBABF_4$. All voltammograms were collected at a scan rate of 5 mV s^{-1}. Five LSVs were collected with a 10 min OCV between scans.

Fc/Fc^+ vs $Ag/Ag(cryptand)^+$ RE

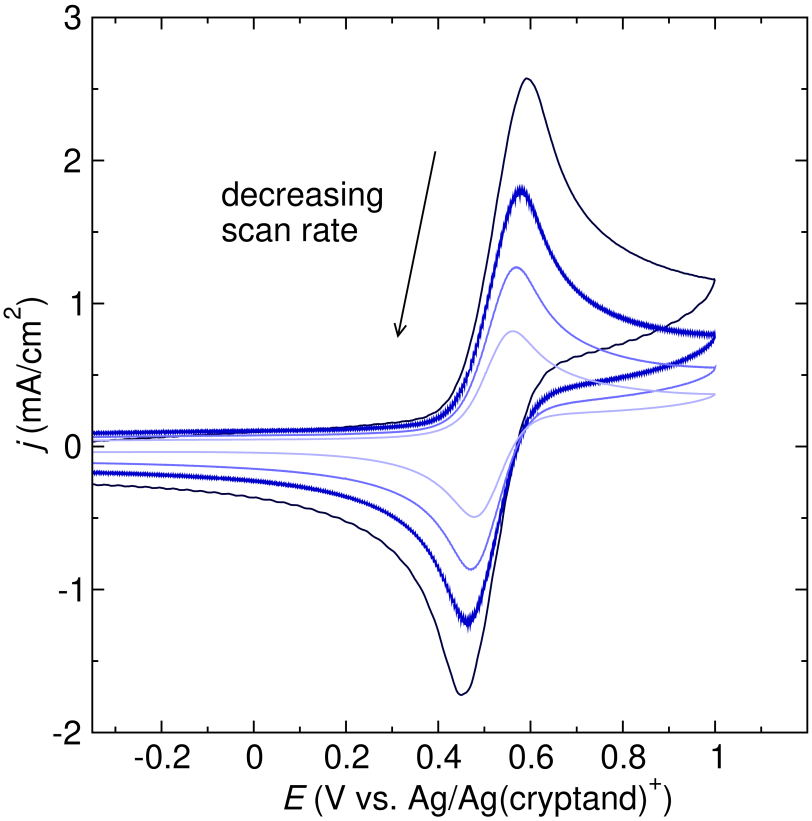

Figure S4: Cyclic voltammograms of Fc in 0.1 M $TBAPF_6$/THF. WE: Pt disk, CE: Pt wire, RE: $Ag/Ag(cryptand)^+$. The voltammograms are collected at 200, 100, 50, and 20 mV s^{-1} scan rate without iR compensation.

EIS data

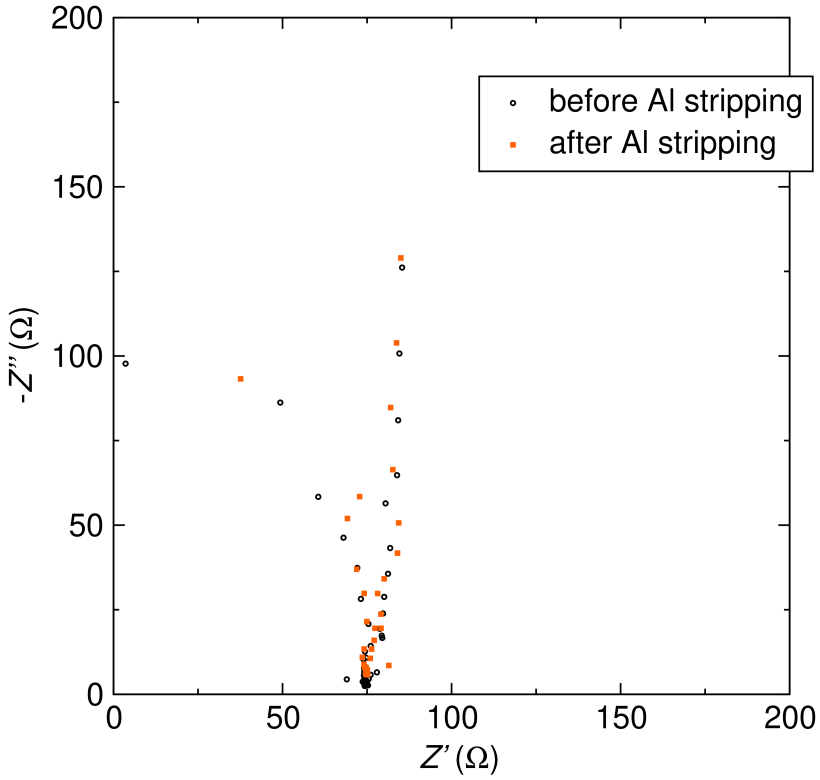

Figure S5: EIS of the Al working electrodes before and after galvanostatic Al stripping in the presence of 0.5 M *t*BuBr in 0.5 M $TBABF_4$ electrolyte.

XPS data

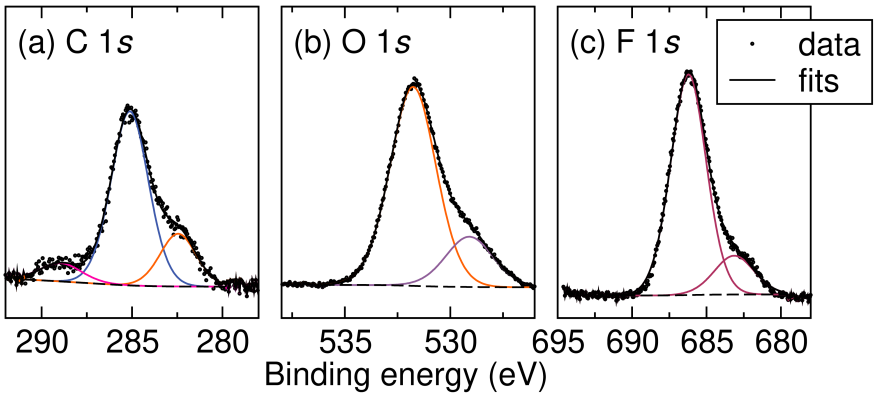

Figure S6: X-ray photoelectron spectra of Al electrodes after the LSV experiments in THF with $TBABF_4$ as the supporting electrolyte.

Table S1: Peak assignments of the X-ray photoelectron spectra of Al electrodes after the LSV experiments in THF with $TBAClO_4$ as the supporting electrolyte.

Figure	**Peak binding energy (eV)**	**Assignment**
Figure 3a. Al 2*p*	72.5	Al^0
	75.1	Al_2O_3
	76.7	AlF_x
Figure S6a. C 1*s*	282.5	C–O
	285.1	adventitious C
	288.9	C=O
Figure S6b. O 1*s*	529.1	Al_2O_3
	531.8	C–O
Figure S6c. F 1*s*	683.1, 686.2	AlF_x

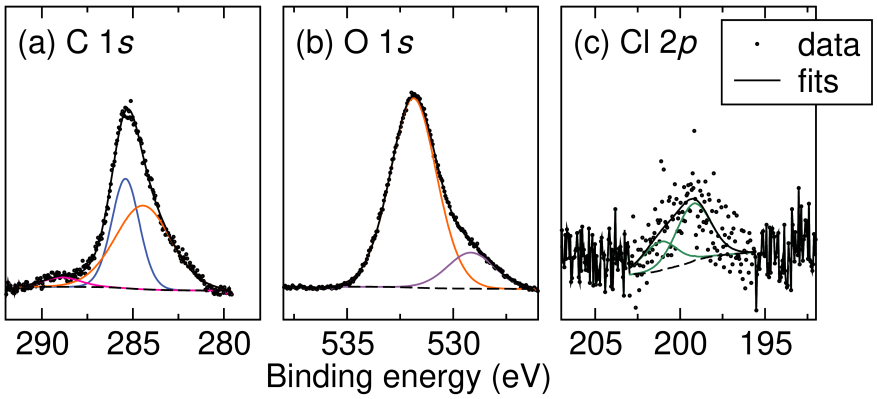

Figure S7: X-ray photoelectron spectra of Al electrodes after the LSV experiments in THF with $TBAClO_4$ as the supporting electrolyte.

Table S2: Peak assignments of the X-ray photoelectron spectra of Al electrodes after the LSV experiments in THF with $TBABF_4$ as the supporting electrolyte.

Figure	**Peak binding energy (eV)**	**Assignment**
Figure 3b. Al 2*p*	72.5	Al^0
	75.0	Al_2O_3
Figure S7a. C 1*s*	284.1	C–O
	285.4	adventitious C
	288.9	C=O
Figure S7b. O 1*s*	529.2	Al_2O_3
	531.9	C–O
Figure S7c. Cl 2*p*	199.2	$AlCl_x$

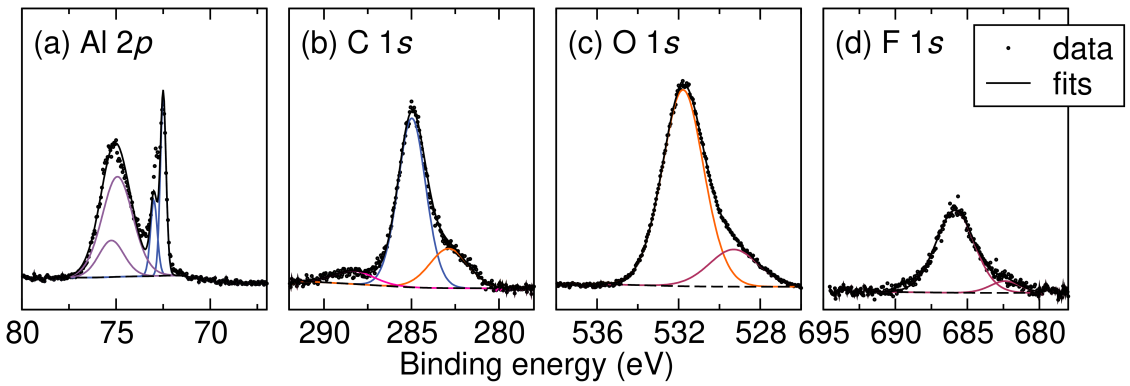

Figure S8: X-ray photoelectron spectra of Al electrodes after the LSV experiments in THF with TBATFSI as the supporting electrolyte.

Table S3: Peak assignments of the X-ray photoelectron spectra of Al electrodes after the LSV experiments in THF with TBATFSI as the supporting electrolyte.

Figure	**Peak binding energy (eV)**	**Assignment**
Figure S8a. Al 2*p*	72.5	Al^0
	75.0	Al_2O_3
Figure S8b. C 1*s*	282.9	C–O
	285.0	adventitious C
	288.3	C=O
Figure S8c. O 1*s*	529.3	Al_2O_3
	531.8	C–O
Figure S8d. F 1*s*	682.4, 685.9	AlF_x

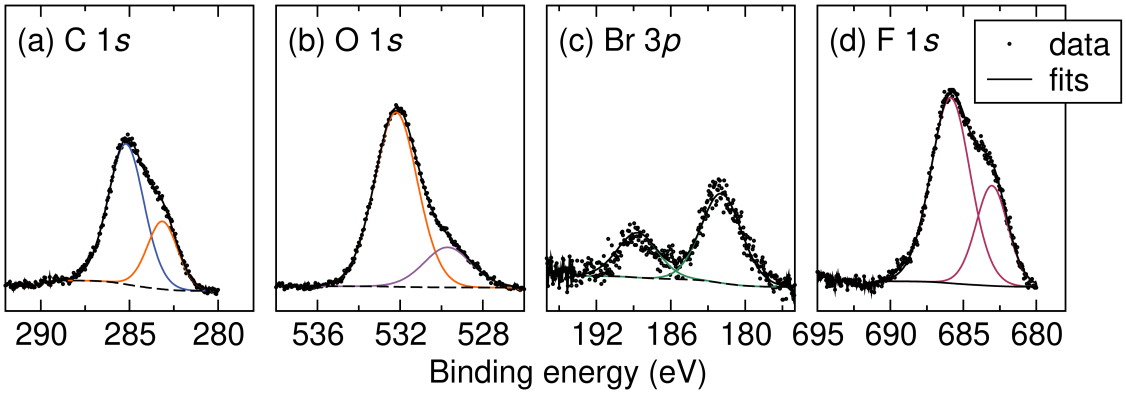

Figure S9: X-ray photoelectron spectra of Al electrodes after the LSV experiments in THF with $TBABF_4$/TBABr as the supporting electrolyte.

Table S4: Peak assignments of the X-ray photoelectron spectra of Al electrodes after the LSV experiments in THF with $TBABF_4$/TBABr as the supporting electrolyte.

Figure	**Peak binding energy (eV)**	**Assignment**
Figure 3c. Al 2*p*	72.5	Al^0
	73.9	$AlBr_3$
	75.0	Al_2O_3
Figure 3c. Br 3*d*	68.4	$AlBr_3$
Figure S9a. C 1*s*	283.1	C–O
	285.2	adventitious C
Figure S9b. O 1*s*	529.7	Al_2O_3
	532.2	C–O
Figure S9c. Br 3*p*	181.9	$AlBr_3$
Figure S9d. F 1*s*	683.0, 685.9	AlF_x

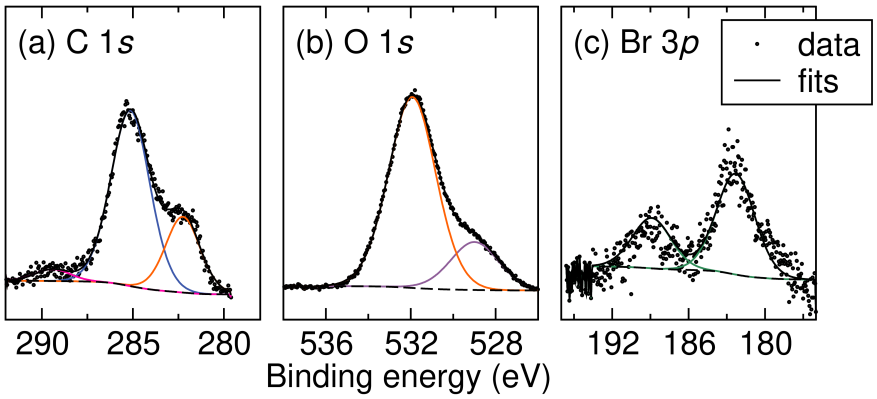

Figure S10: X-ray photoelectron spectra of Al electrodes after the LSV experiments in THF with $TBAClO_4$/TBABr as the supporting electrolyte.

Table S5: Peak assignments of the X-ray photoelectron spectra of Al electrodes after the LSV experiments in THF with $TBAClO_4$/TBABr as the supporting electrolyte.

Figure	**Peak binding energy (eV)**	**Assignment**
Figure 3d. Al 2*p*	72.5	Al^0
	73.8	$AlBr_3$
	75.1	Al_2O_3
Figure 3d. Br 3*d*	68.8	$AlBr_3$
Figure S10a. C 1*s*	282.2	C–O
	285.1	adventitious C
	289.4	C=O
Figure S10b. O 1*s*	529.7	Al_2O_3
	532.2	C–O
Figure S10c. Br 3*p*	182.3	$AlBr_3$

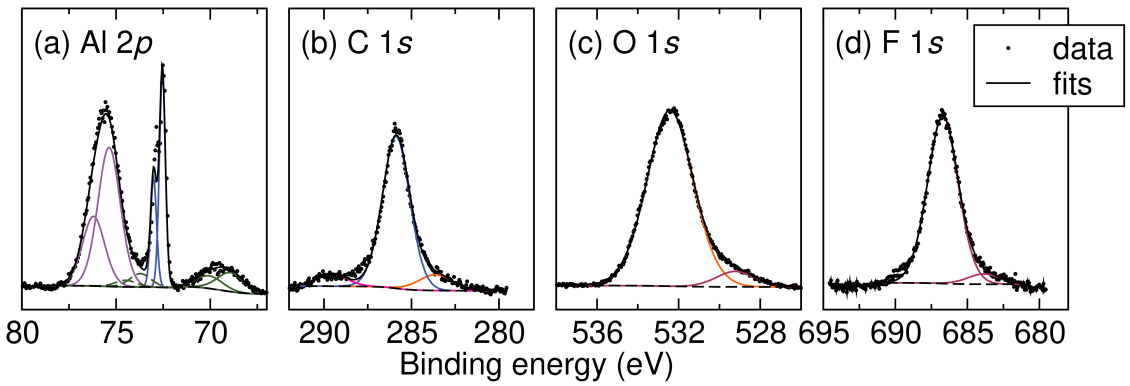

Figure S11: X-ray photoelectron spectra of Al electrodes after the LSV experiments in THF with TBATFSI/TBABr as the supporting electrolyte.

Table S6: Peak assignments of the X-ray photoelectron spectra of Al electrodes after the LSV experiments in THF with TBATFSI/TBABr as the supporting electrolyte.

Figure	**Peak binding energy (eV)**	**Assignment**
Figure S13a. Al 2*p*	72.5	Al^0
	73.7	$AlBr_3$
	75.4	Al_2O_3
Figure S13a. Br 3*d*	68.9	$AlBr_3$
Figure S13b. C 1*s*	283.6	C–O
	285.8	adventitious C
	289.6	C=O
Figure S13c. O 1*s*	529.2	Al_2O_3
	532.4	C–O
Figure S13d. F 1*s*	683.8, 686.7	AlF_x

NMR data

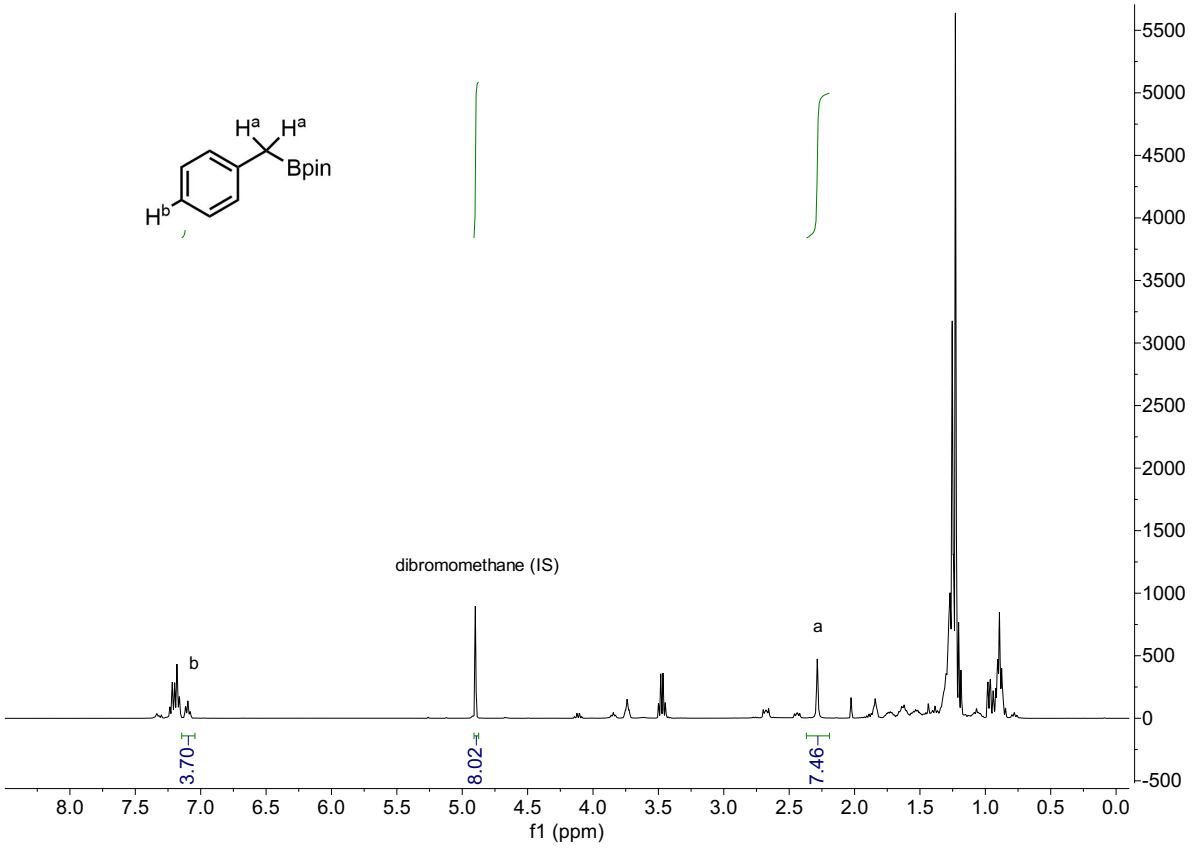

Figure S12: An example of the ^{1}H-NMR spectra of the borylation reaction crude mixture.

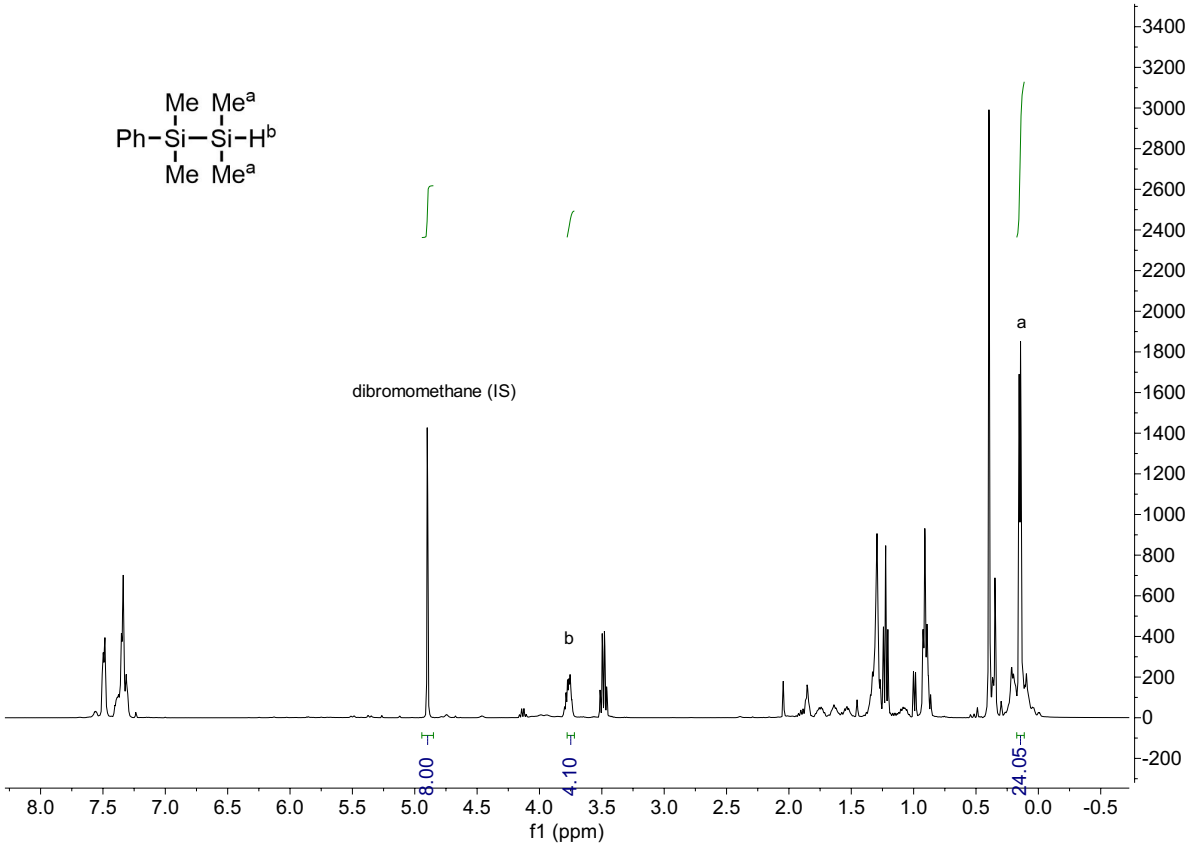

Figure S13: An example of the ^{1}H-NMR spectra of the silylation reaction crude mixture.